An alternative approach to recover lead, silver and gold from Black Gossan (polymetallic ore). Study of biological oxidation and lead recovery stages

Juan Lorenzo-Tallafigo*, Nieves Iglesias-González, Alfonso Mazuelos, Rafael Romero, Francisco Carranza

E-mail addresses:

Juan Lorenzo-Tallafigo*: jualortal@alum.us.es (Corresponding author)

Nieves Iglesias-González: mnieves@us.es

Alfonso Mazuelos: mazuelos@us.es

Rafael Romero: aleta@us.es

Francisco Carranza: fcarranza@us.es

Affiliation: Chemical Engineering Department, Universidad de Sevilla, Calle Profesor García González s/n, 41012 Sevilla, Spain.

Word count: 7943 words

Keywords

Biomining

Jarosite dissolution

Citrate leaching

Polymetallic ore

Lead recovery

Highlights

An alternative approach is proposed to recover Pb, Ag and Au from sulphide ores

For first time citrate leaching of a biooxidation residue is studied

A H_2SO_4 washing of bioleaching residue enhances Pb recovery in citrate leaching

Temperature and H_2SO_4 concentration are the mandatory variables in acid washing

pH and pulp density play a key role in the citrate leaching

Graphical Abstract

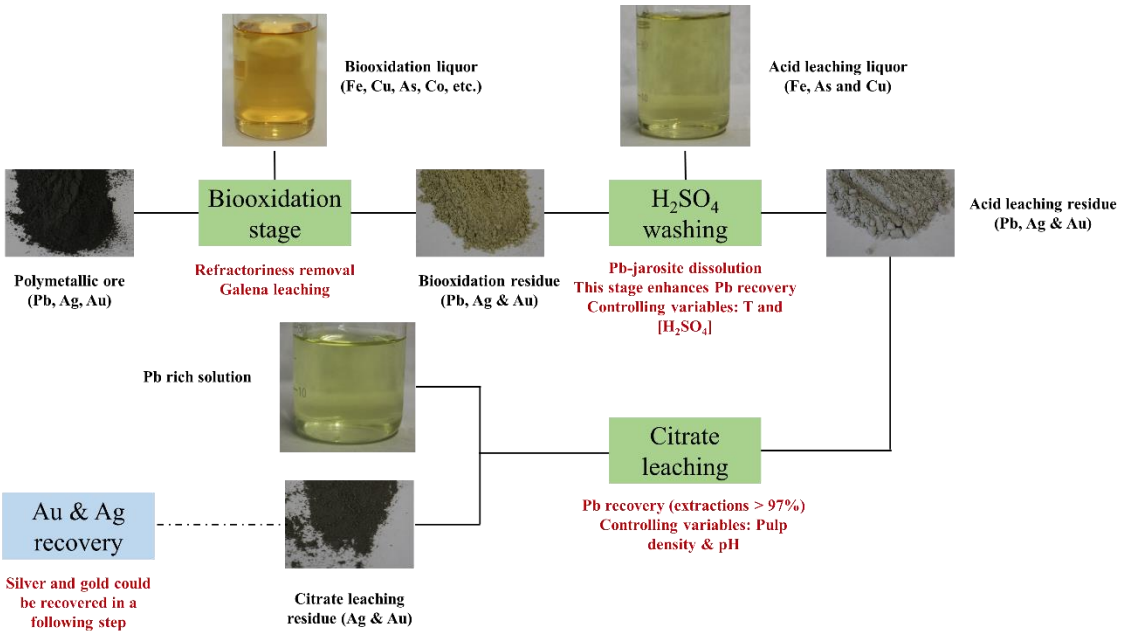

ABSTRACT

A novel procedure to recover lead, silver and gold from polymetallic sulphide ores, cleaner than the traditional hydrometallurgical route (hot brine leaching), is proposed. This process consists of a biooxidation stage, where sulphides are oxidised by the action of extremophiles, followed by an acid washing and a citrate leaching in which lead is recovered. The final solid obtained, mainly composed of quartz, is rich in silver and gold. This paper is focused on the biooxidation and the lead recovery of the black gossan, a polymetallic sulphide ore with valuable amounts of lead, silver and gold. Biooxidation performed with a mixed mesophilic culture (mainly *Acidithiobacillus ferrooxidans*) at 20% pulp density is able to dissolve the sulphide matrix, removing the gold refractory behaviour and producing jarosite, beaverite, gypsum and anglesite. A previous sulphuric acid washing of biooxidation residue greatly improves the lead recovery in the citrate stage. In the sulphuric acid washing, jarosite and beaverite are dissolved, being the most important variables the temperature and sulphuric acid concentration. The jarosite dissolution kinetics shows that the rate controlling step is the chemical reaction, with an activation energy of 86.4kJ/mol. A linear relationship between the jarosite dissolved and lead recovered is found, reinforcing the necessity of a previous H_2SO_4 washing. The optimal pH range for lead recovery in the citrate solution is 5-9. Pulp densities higher than 5% produces an unstable solution, precipitating a part of the lead. A negative effect of gypsum has been confirmed through several citrate leaching tests performed with pure anglesite. The solid obtained after the studied stages is suitable to recover gold and silver that contains.

1. Introduction

Polymetallic ores, specially sulphide minerals, such as pyrite (FeS_2) or galena (PbS), are the major sources for recovery of associated metal values such as gold and silver, and other base metals (Schippers et al., 2013). Recently, several factors are affecting the metal production, such as the discovery of ore deposits that are more difficult to exploit (complex mineralogy), a decrease in the grade of minerals, longer and more difficult environmental permitting process, higher capital and operating costs, and technological challenges. These changes drive to need for technological innovation, and specially biomining (Brierley, 2008; Norgate and Jahanshahi, 2010).

These polymetallic and low-grade ores are uneconomical to be treated by conventional metallurgical techniques, in contrast with the biohydrometallurgical technologies that have the potential to benefit them. Besides, bioleaching is more environmentally benign approach than traditional pyrometallurgical processes, as no SO_2 is generated, arsenic is fixed in a stable precipitate, and is able to dissolve the pyrite matrix in refractory gold and silver ores (Fomchenko et al., 2016; Kaksonen et al., 2014; Choi et al., 2018). A case of these polymetallic ores is the black gossan found in Las Cruces Mine (Spain). This ore, mainly composed of sulphides and calcite ($CaCO_3$), contains valuable amounts of lead, silver and gold. Tornos et al. (2014) reported 3.85 g/t of gold, 109 g/t of silver and 8.7% of lead in black gossan.

Hot brine leaching (HBL) to recover Pb, Ag and Au, especially from mining waste, is the process more widely studied. In the case of gold recovery, an oxidising agent is necessary to provide an oxidation reduction potential (ORP) higher than 900 mV, some relevant studies found in the literature are Viñals et al. (1991), Frías et al. (2002), Behnajady and Moghaddam (2014) and Nesbitt et al. (1990). If Pb, Ag and Au are contained in a sulphide matrix, a previous step to dissolve the matrix will be necessary because Pb is found as PbS, and Au and Ag are occluded (Eymery and Ylli, 2000; Iglesias and Carranza, 1994). This pretreatment can be varied, such as roasting (Dunn and Chamberlain, 1997), pressure oxidation (Gudyanga et al., 1999), biooxidation (Fomchenko et al., 2016; Mubarok et al., 2017) or alkaline sulphide leaching (Celep et al., 2011).

The implementation of HBL to dissolve the valuable metals (Ag, Au and Pb) from biooxidation residues could present some troubles:

- Chloride medium increases the industrial costs due to equipment corrosion (Gómez et al., 1997).
- Jarosite formed in bioleaching stage will be dissolved in an acid chloride medium forming a $FeCl_3$ dissolution that has environmental problems.
- Gold recovery in chloride media needs an oxidising agent, usually hypochlorite, which at pH values lower than 3.5 forms chlorine (Cl_2), and an acid medium is required to stabilise the lead chloride complex formed. Therefore, the simultaneous recovery of lead and gold will be complicated, leading to the chlorine formation, with environmental problems, or to lower lead recoveries (Nesbitt et al., 1990; Behnajady and Moghaddam, 2014).
- The addition of calcium hypochlorite could promote the co-precipitation of anglesite ($PbSO_4$) and gypsum ($CaSO_4 \cdot 2H_2O$) (Behnajady and Moghaddam, 2014).

For these reasons an alternative hydrometallurgical process is proposed to recover Pb, Ag and Au from sulphide ores, mainly FeS_2. This proposal (Fig. 1) consists of a biological stage to oxidise the sulphide minerals, a second step to extract Pb from solid residue using softer conditions than HBL, and a third stage where Ag and Au are recovered. The optimisation in the Pb, Ag and Au recovery in each stage is sought, as well as, the replacement of the HBL by the proposed novel hydrometallurgical technology to recover these target metals.

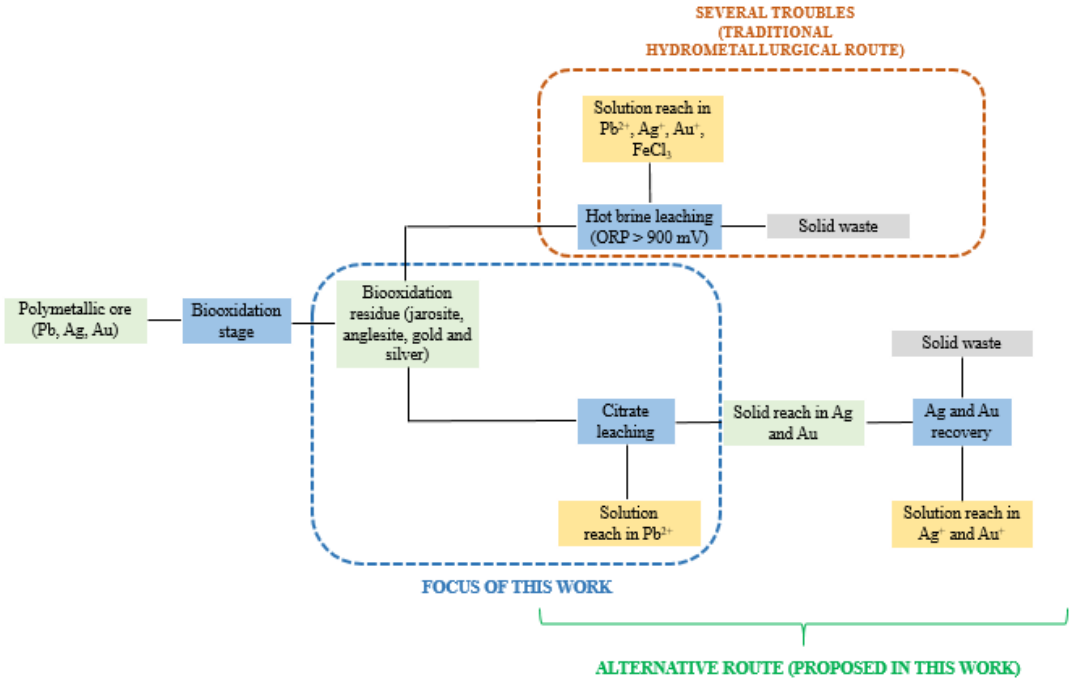

Fig. 1: Alternative hydrometallurgical process to recover Pb, Au and Ag from sulphide ores against hot brine leaching.

From a conceptual point of view, the first stage of this process is the sulphides oxidation, through biooxidation with extremophilic microorganisms. Biomining is an efficient technology to remove the refractoriness of these ores and to oxidise the lead sulphide (Mubarok et al., 2017; Fomchenko et al., 2016; Mahmoud et al., 2017). Reactions that take place in the biooxidation stage are the following (r1-r8):

$$2\,FeS_2(s) + 7O_2 + 2H_2O \xrightarrow{\text{bacteria}} 2Fe^{2+} + 4SO_4^{2-} + 4H^+ \text{ (r1)}$$

$$Fe^{2+} + {}^1/_4\,O_2 + H^+ \xrightarrow{\text{bacteria}} Fe^{3+} + {}^1/_2\,H_2O \text{ (r2)}$$

$$1/8\,S_8(s) + {}^3/_2\,O_2 + H_2O \xrightarrow{\text{bacteria}} SO_4^{2-} + 2H^+ \text{ (r3)}$$

$$PbS\,(s) + 2Fe^{3+} \rightarrow Pb^{2+} + 2Fe^{2+} + S^0(s) \text{ (r4)}$$

$$Pb^{2+} + SO_4^{2-} \rightarrow PbSO_4(s) \text{ (r5)}$$

$$M^+ + 3Fe^{3+} + 2SO_4^{2-} + 6H_2O \rightarrow MFe_3(SO_4)_2OH_6(s) + 6H^+ \text{ (r6)}$$

r1-r3 (Iglesias and Carranza, 1994) are reactions catalysed by bacteria, pyrite dissolution, ferric ion regeneration and elemental sulphur oxidation, respectively. r4 is the indirect bioleaching of galena, being this reaction strongly dependent of ferric ion

generated by r2. According to r5, the dissolved Pb^{2+} precipitates in sulphate medium remaining in the solid residue (Palencia et al., 1989). In the biooxidation processes usually precipitates jarosite ($MFe_3(SO_4)_2OH_6$) due to the presence of ferric ion, sulphate ion and a monovalent ion ($M^+ = K^+$, NH_4^+, Na^+, H^+ or Ag^+), and occasionally a divalent cation such as Pb^{2+} (r6) (Patiño et al., 1994). Jarosite formation could catch the target metals, such as Pb^{2+} and Ag^+, and difficult the metal recovery (Patiño et al., 1994; Kasaini et al., 2000). In addition, $CaCO_3$ is dissolved in an acid medium (r7), producing CO_2 and Ca^{2+}, that precipitates, in a sulphate medium, as $CaSO_4 \cdot H_2O$ (r8).

$$CaCO_3(s) + 2H^+ \rightarrow Ca^{2+} + CO_2(g) + H_2O \quad \text{(r7)}$$

$$Ca^{2+} + SO_4^{2-} + 2H_2O \rightarrow CaSO_4 \cdot 2H_2O(s) \quad \text{(r8)}$$

Leaching with sodium citrate ($Na_3C_6H_5O_7$) for the recovery of lead from bioleaching solid waste could be an alternative approach regarding HBL. Lead leaching in citrate solution has been mostly studied in pure anglesite (Zárate-Gutiérrez and Lapidus, 2014), in secondary lead smelting (Kim et al., 2017) and in spent lead acid battery paste (Zhu et al., 2013; Zhang et al., 2016; Sonmez and Kumar, 2009). Nevertheless, this leaching process could be applied to solid waste from galena leaching, where the majority lead species will be anglesite and beaverite ($Pb(Fe_2Cu)(SO_4)_2(OH)_6$). This procedure offers softer conditions than hot brine solutions, such as room temperature or pH close to 7. The citrate leaching of anglesite can be represented by the following reaction (r9) (Kim et al., 2017).

$$3PbSO_4 + 2Na_3C_6H_5O_7 \cdot 2H_2O \rightarrow Pb_3(C_6H_5O_7)_2 \cdot 3H_2O + 3Na_2SO_4 \quad \text{(r9)}$$

However, r9 shows a strong dependence on pH, forming different lead and citrate ion (cit^{3-}) complexes between pH 4.6 and 11.6, such as $Pb(Cit)_2^{4-}$, $Pb(HCit)(Cit)^{3-}$, $Pb(Cit)^-$, $Pb_2(Cit)_2^{2-}$ or $Pb_2(Cit)_2(OH)_2^{4-}$, where (Cit) is $(C_6H_5O_7)^{3-}$ (Zárate-Gutiérrez and Lapidus, 2014).

After biooxidation and lead recovery, the solid waste could present valuable amount of gold and silver that could be recovered in a following step. Cyanide leaching is the most common process for gold recovery and it has widely been studied in biooxidation solid waste (Amankwah et al., 2005; Mubarok et al., 2017; Fomchenko et al., 2016), nevertheless due to the growing environmental concern of the use of cyanide, this process is becoming more restricting. Recently, two alternative processes have been

studied to replace the cyanide solutions, the hypochlorite-chloride (Hasab et al., 2013a; Hasab et al., 2013b; Jeffrey et al., 2001; Hasab et al., 2014) and thiosulphate (Webster, 1984; Fleming et al., 2003; Melashvili et al., 2016; Xu et al., 2016; Celep et al., 2018; Jeffrey et al., 2001) leaching. These processes have been directly applied in refractory gold ores and in pressure leaching wastes, but these techniques have not been applied in biooxidation residues yet.

The aim of this work is the study of a novel approach to recover Pb, Ag and Au from sulphide ores, avoiding the use of hot brine solutions. The proposed treatment has been tested with the black gossan, because this one is a polymetallic ore with valuable amounts of Pb, Ag and Au, and important amounts of sulphides, being an appropriate ore to study this new approach. The study is focused on the biological stage and on the citrate leaching of lead.

2. Materials and methods

2.1 Analytical methods

2.1.1 Metals measurement

Fe, Cu, Zn, Ag, Pb, Sb, As, Co, In, Ca, Na and K were analysed by atomic absorption spectrophotometry (AAS), Perkin Elmer 2380 Model (United states). These metals were determined in the solutions and in the solids, to measure the metals in solid a previous acid digestion (3HCl: 1HNO_3) of a known mass amount was performed.

Au was determined in the solid samples by the fire-assay technique. This technique consists of a fusion at 900 ºC, followed by a cupellation at 1000 ºC, and an acid digestion to determine Au by AAS.

Ferrous ion was determined in biooxidation solutions through a redox titration with potassium dichromate ($K_2Cr_2O_7$). These measurements were performed with an automatic titrator, TTT80 model Radiometer Copenhagen (Denmark).

2.1.2 X-ray diffraction (XRD)

XRD analysis were performed under the following conditions: $Cu_{k\alpha 1}$ = 1.5418 Å and 2θ from 3.0 to 70.0º. These analyses were carried out in CITIUS (Centro de Investigación, Tecnología e Innovación de la Universidad de Sevilla) with a powder diffractometer (Bruker D8 model advance A25, United States). The different compounds were determined with the DIFFRAC.EVA software (Bruker, United States).

2.1.3 Granulometric analysis

Particle size distribution were determined by laser diffraction, using the Beckman Coulter LS 13-320-MW model (United States). The analyses were carried out with a disaggregant and with an obscurance of 8-10%.

2.1.4 Total reflection X-ray fluorescence (TXRF)

These analyses were carried out in CITIUS with a Bruker fluorescence spectrometer S2 PICOFOX model (United States), under the following conditions: Mo_k ,600 µA, 50 kV, a live time = 500s and dead time = 12.3%.

2.1.5 Diagnostic cyanide leaching

Cyanidation was carried out in a cylindrical 1L-reactor, mechanical agitation fixed to 300 rpm, aerated, with 2000 ppm NaCN, 20% of pulp density and a pH value of 12. After 24 hours, the stirred was filtered and gold was determined in the solid residue.

2.2 Black Gossan

The black gossan, found in Las Cruces Mine (Spain), was studied in this work. Table 1 shows the chemical composition of the black gossan, notice the valuable grade in Pb, Ag and Au. Fig. 2A presents the XRD pattern of this ore, where pyrite, calcite, galena and quartz were identified. From the chemical composition and the identified minerals, the mineralogical composition, shown in Table 2, was determined. Calcite is the main compound, followed by important amounts of metal sulphides (pyrite and galena). Table 3 shows the granulometric data of the black gossan.

1 Table 1: Chemical composition of the black gossan, the bioleaching solid residue and the acid leaching
2 solid residue.

Material	Black Gossan	Biooxidation residue	Acid washing residue
Fe (%)	16.62	9.45	1.96
Pb (%)	9.15	7.05	11.03
Ca (%)	18.98	14.61	13.3
Cu (%)	0.43	0.21	0.03
Zn (%)	0.13	0.07	0.07
K (%)	-	0.27	-
Na (%)	-	0.97	-
Au (ppm)	3.32	2.43	3.83
Ag (ppm)	195	167	263
In (ppm)	49	44	39
Co (ppm)	95	-	-
Sb (ppm)	2388	1628	1840
As (ppm)	5300	3143	-

3

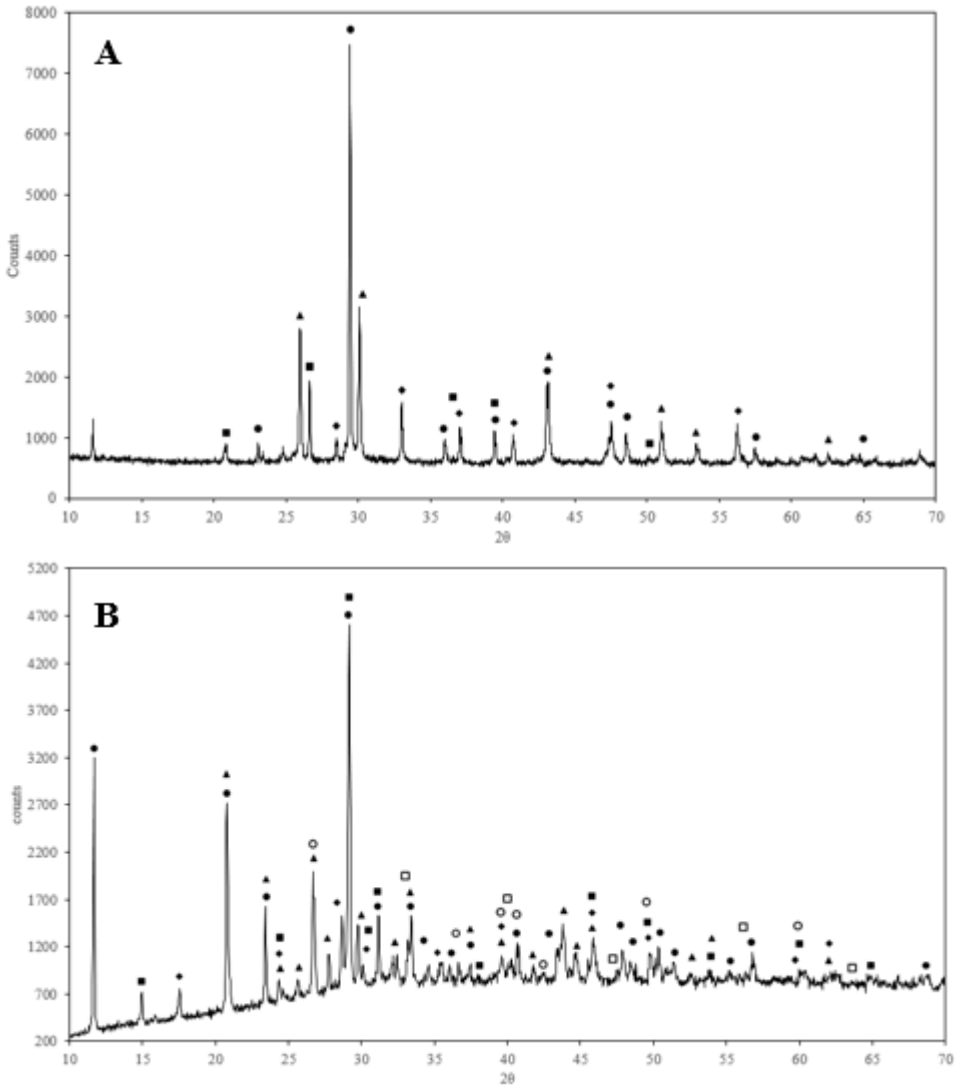

Fig. 2: XRD pattern of the black gossan (● = calcite, ▲= galena, ♦ = pyrite and ■ = quartz) (A). XRD pattern of the biooxidation solid residue (○ = Quartz, □ = pyrite, ♦ = hydronian jarosite, ■ = Beaverite (Cu), ▲ = Anglesite and ● = gypsum) (B).

.

Table 2: Mineralogical composition of the black gossan, the bioleaching solid residue and the acid leaching solid residue (* quartz is not determined in acid digestion)

Compound	Black gossan	Biooxidation residue	Acid washing residue
Calcite (%)	47.38	-	-
Galena (%)	10.56	-	-
Pyrite (%)	35.65	2.67	4.20
Gypsum (%)	-	62.71	57.09
Anglesite (%)	-	6.19	16.14
Jarosite, as hydronian jarosite (%)	-	10.06	-
Beaverite (%)	-	15.38	-
Total (%)	93.59	97.01	77.43*

Table 3: Granulometric data determined by laser diffraction of black gossan, bioleaching solid residue and acid leaching solid residue (DX= maximum diameter of X% of particles).

Material	D20 (µm)	D50 (µm)	D80 (µm)	Mean diameter (µm)
Black gossan	3.9	13.5	27.7	16.8
Biooxidation residue	1.7	10.5	18.1	10.4
Acid washing residue	2.1	10.4	20.5	12.0

2.3 Experimental

2.3.1 Biooxidation tests

Preliminary tests (Fig. S1-S5) were performed in order to select the experimental conditions in biooxidation. Mahmoud et al, 2017 reported optimal conditions for bacterial growth of *Acidithiobacillus ferrooxidans* $1.8 \leq pH \leq 2.5$ and 30-35° C. High values of pulp density have a double negative effect on bioleaching, on the one hand the high content of calcite increases the pH, and on the other hand, in the absence of calcite, the acid generated by r1 causes it to drop, in both cases this variable is outside the optimal range. Preliminary tests show there is no influence of inoculum percentage or particle size below 150 µm.

2.3.1.1 Inoculum preparation

A mixed culture mainly consists of *Acidithiobacillus ferrooxidans* (FNN) was used in this study. This culture is routinely maintained in the exponential growth phase by successive subculturing in 9K medium (Silverman and Lundgren, 1959) every 48h.

A 4-L culture was prepared in a stirred bioreactor adding 20% of FNN and 80% of 9K medium without ferrous iron. In order to adapt bacteria to gossan, it was incorporated progressively from a 2% to 20% of pulp density. The bioreactor was mechanically stirred at 500 rpm and aerated (1.13 L/min). During the course of the culture, pH and ORP (calomel reference electrode) were measured, temperature was maintained at 30°C. As the ore is rich in limestone, the acid generated by pyrite dissolution is neutralised. The criterion for the addition of more mineral was that there was no pH variation.

2.3.1.2 Biooxidation test at high pulp density

Bioleaching test at 20% of pulp density (w/v) was carried in cylindrical 6L-bioreactor mechanically stirred (500 rpm) at 30°C, maintained at pH 2 and aerated (1.13 L/min). 800 g of pulp from the culture described in section 2.3.1.1, 3200 g of 9K medium without ferrous iron and 800 g of gossan were placed in the bioreactor. Target pH=2 was adjusted with 0.5M H_2SO_4 to neutralise limestone and was maintained with 2M NaOH during the culture.

The fraction of pyrite converted (α) is calculated from eq. 1.

$$\alpha = \text{pyrite}_o(g) - \text{pyrite}_t(g)/\text{pyrite}_o(g) \quad \text{(eq. 1)}$$

where pyrite_o is the initial amount of pyrite and pyrite_t is the amount of pyrite at time t. As in bioleaching process pyrite dissolution generates ferrous iron (r1) that is biooxidised to ferric iron (r2) and is partially precipitated as jarosite (r6), the amount of pyrite at time t is determined as follows: At different times, a sample of pulp is extracted from the reactor by means of a syringe. The sample is weighed and filtered. Total iron and ferrous iron are analysed in the filtrate, and the solid is treated with 1M HCl to dissolve the jarosite. After filtering, the solid is attacked with aqua regia and the pyrite content is determined by iron analysis.

2.3.2 Acid washing tests

Two types of jarosite are present in the biooxidation residue, hydronian jarosite and beaverite, both are dissolved in the acid washing. The parameter to characterise these tests is the jarosite dissolution (α), calculated from the iron dissolved belonging to hydronian jarosite and beaverite compounds. In order to calculate Fe belonging to the jarosite, a determined mass of biooxidation residue was treated with 1M HCl, when jarosite was dissolved the pulp was filtered and Fe in the solution and remaining in solid

was determined (Reyes et al., 2017). Fe from solution is associated to jarosite. From eq. 2, jarosite dissolution in these tests were calculated.

$$\text{Jarosite dissolution } (\alpha) = \frac{\text{Fe}_i(\%)/100 \cdot \text{initial mass (g)} - \text{Fe}_f(\%)/100 \cdot \text{final mass (g)}}{\text{Fe}_{\text{jarosite}}(\%)/100 \cdot \text{initial mass(g)}} \qquad \text{(eq. 2)}$$

Being Fe_i (%), Fe_f (%) and $Fe_{jarosite}$ (%) the iron grade of the added mass, the acid washing residue and the belonging to the jarosite of the added mass, respectively. The initial mass is the solid amount added to test and the final mass is the residue amount after acid washing.

2.3.2.1 Erlenmeyer flask tests

Tests performed to study the variables (sulphuric acid concentration, temperature, time and pup density) that are involved in the acid dissolution of jarosite were carried out in Erlenmeyer flasks (250mL) placed in a magnetic stirrer fitted with a heating plate. Acid washing liquors were prepared from commercial sulphuric acid (98%) (PANREAC) and distilled water. Washing dissolution was heated to the working target temperature and later a determined mass of biooxidation residue was added to the flask. At the end of the test the pulp was filtered, and Fe was measured from dissolution. From solid residues, weight loss was calculated, and Fe remaining in the solid was measured, previous acid digestion.

In tests where the jarosite dissolution was obtained with respect time, samples of a known volume were withdrawn and filtered. In these liquid samples Fe was determined.

2.3.2.2 Stirred tank reactor tests

Once the variables for the jarosite dissolution were selected, two acid leaching tests were performed in a cylindrical 6L-reactor, with mechanical agitation fixed to 500 rpm, 3 deflectors and a heat exchanger connected to a thermostat. The experimental conditions are the following: 180 min, 8% pulp density, 90 g/L H_2SO_4 and 80 ºC. As in section 2.3.2.1, when the leaching liquor reached the experimental temperature a known mass of bioleaching residue was added. At the end of the test, the pulp was filtered and Cu, Zn, Fe, Ca, Co, In, Pb, Ag, K, Na, As and Sb were measured in the leaching liquor and the solid residue.

2.3.3 Citrate leaching tests

Citrate leaching tests were carried out in Erlenmeyer flasks, magnetically stirred and at room temperature. Citrate dissolutions were prepared from sodium citrate tribasic dihydrate (≥99.0%) (FLUKA) and distilled water. A determined mass of solid was added to citrate solution, and then pH was adjusted with diluted sulphuric acid or sodium hydroxide. When pH was adjusted to the target pH the test started. After the experiment, pulp was filtered and from solid residue the weight loss was calculated and Pb and Ca were determined.

2.4 Kinetics

The kinetics of biooxidation at 20% pulp density and of the acid washing at different temperatures were studied. Eqs. 3-6 were used to describe the experiments. These equations describe solid-liquid reactions where the rate controlling step is the chemical reaction in the solid surface. Eq. 3 describes the shrinking core model where a passivating film is not formed, eq. 4 and eq. 5 are kinetic equations as a function of the kinetic order with respect solid phase, first and second order, respectively. Eq. 6 is the Arrhenius equation where the kinetic constant (k) is related with the experimental temperature (T) to obtain the activation energy (Ea).

$$1 - (1 - \alpha)^{\frac{1}{3}} = kt \quad \text{(eq. 3)}$$

$$-\ln(1 - \alpha) = kt \quad \text{(eq. 4)}$$

$$(1 - \alpha)^{-1} = kt \quad \text{(eq. 5)}$$

$$k = A \cdot e^{-Ea/RT} \rightarrow \ln k = \frac{Ea}{R} \cdot \frac{1}{T} + A \quad \text{(eq. 6)}$$

Being t the time, α the reaction conversion, k the kinetic constant (d^{-1}), A the preexponential factor, T the experimental temperature (K), Ea the activation energy (kJ/mol) and the R the gas constant (R = 8314 $kJ \cdot mol^{-1} \cdot K^{-1}$).

3. Results and discussions

3.1 Biooxidation at high pulp density

Fig. 3 shows data of biooxidation at 20% of pulp density, pH = 2 and 30°C. Fig.3A presents the evolution of ferrous and ferric iron. At the beginning, ferric iron concentration falls due to carbonate dissolution that causes ferric ion precipitation,

which corresponds to ORP drop to 430 mV observed in Fig. 3B, and to an increase in pulp density showed in Fig. 3C. Ferrous iron concentration increases until to reach a maximum to fall to 0. Ferric ion concentration and ORP (Fig. 3B) increase with the same trend until approximately 30 days when both decrease due to jarosite precipitation. The precipitation of jarosite causes an increment in pulp density as can be observed in Fig.3C.

Fig. 3B shows the NaOH consumption (g NaOH/ g ore) versus time. There is no NaOH addition in the first 10 days because the gossan contains a 47.4% of calcite that neutralises the acid generated by pyrite oxidation. The total consumption was 212 g of NaOH per kg of gossan. In a continuous operation, alkali consumption would be lower because part of the generated acid would be neutralised by the calcite-bearing gossan feed. Fig. 3D shows the pyrite conversion during the culture, reaching a 95% after 45 days of biooxidation. As it is shown in Fig. 3D, experimental data fits well (R^2=0.9877) shrinking core model with chemical control (eq.3). This model, with a kinetic constant k=0.0151 d^{-1}, predicts a time of 66.2 days to deplete all the substrate.

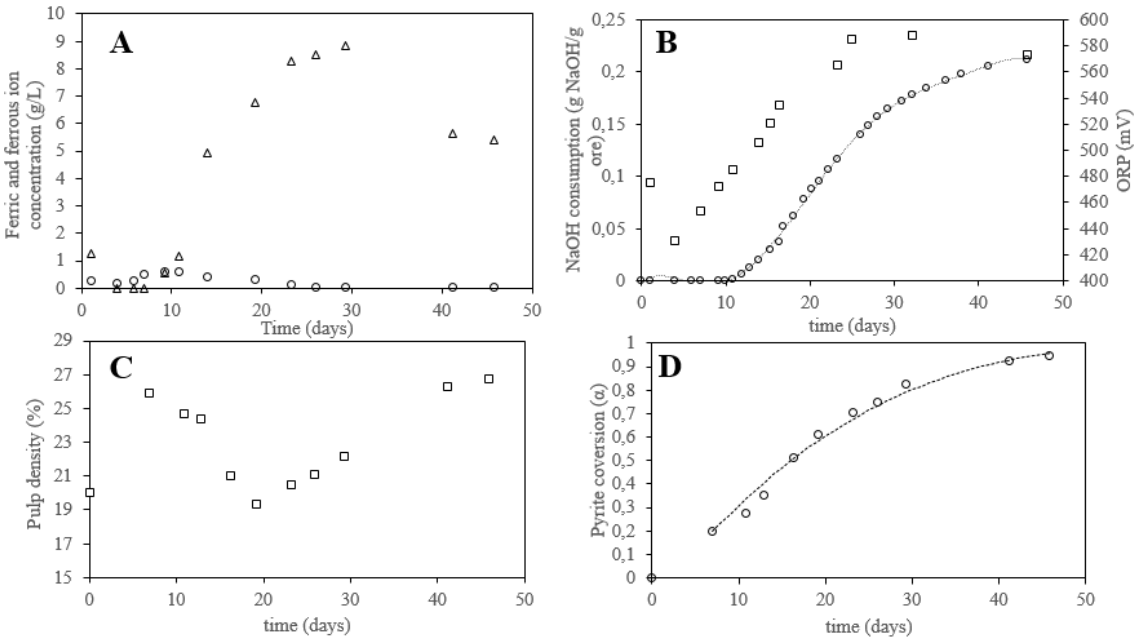

Fig. 3: Results obtained in biooxidation tests. Ferric and ferrous ion (g/L) evolution (▲ = Ferric ion and ○ = ferrous ion) (A), NaOH consumption (g NaOH/ g ore) (○) and ORP (mV) (□) (B), pulp density (□) variation as a function of biooxidation time (C), and pyrite conversion evolution (○) and fit of kinetic eq. 2 (line) (D).

The semi-logarithmic plot of substrate consumption (Ln([pyrite]$_o$-[pyrite]) versus time, is a straight line (R^2= 0.991) whose slope, the specific bio-oxidation pyrite rate, is 0.096 d^{-1} (0.004 h^{-1}). The composition of biooxidation liquor after 45.8 is the following: 240 ppm Cu, 61 ppm Zn, 5410 ppm Fe, 8.7 ppm Co, 1.3 ppm In, 274 ppm Ca, 200 ppm As and 37.5 ppm Sb.

After biooxidation process, the solid mass is increased by 36.8 % in relation to the initial value, due to the precipitation of gypsum, anglesite, hydronium jarosite ($(H_3O)Fe_3(SO_4)_2(OH)_6$ and beaverite, species identified, together with quartz and pyrite, by XRD in the solid bioleaching residue (Fig. 2B). Anglesite and beaverite are the two phases where lead is retained. Beaverite has the jarosite structure where the monovalent cation (M^+) is replaced by a Pb^{2+} ion and a Fe^{3+} ion is replaced by a Cu^{2+} ion. In Table 1, the chemical composition of the solid residue and the black gossan can be compared. The content in Pb, Ag and Ca has decreased, even though these elements remain mostly in the residue, due to the increase in mass.

In order to observe the refractoriness removal, diagnostic cyanide leaching of black gossan and the biooxidation residue were performed. Gold recovery after cyanidation of the biooxidation residue was of 86.4%, this extraction is much higher than the gold recovery reached in the direct cyanidation of black gossan (17.3%). In view of these results, it can be confirmed that the biooxidation stage has removed the refractory behaviour and the precious metals could be extracted in a subsequent step.

3.2 Lead recovery

3.2.1 Preliminary citrate tests

Lead, silver and gold remain in the biooxidation solid residue (Table 1**)**. Several citrate leaching tests were performed so as to evaluate the lead extraction from the biooxidation solid residue. The sodium citrate concentration, pH value and time of preliminary tests (PT) were selected according to Zárate-Gutíerrez and Lapidus (2014). Table 4 shows the experimental conditions and Pb recoveries for each experiment. In PT-1 and PT-2 solid biooxidation residue was directly added to citrate solution reaching low lead recoveries in both of them. After observing the low extraction in PT-1, a second preliminary test (PT-2) was performed increasing the reaction time, from 2 to 16 hours, and decreasing the pulp density, from 2 to 1. However Pb extraction increases slightly from 41.2 (PT-1) to 49.2 (PT-2). These results make evident a refractory

behaviour with respect citrate leaching that could be caused by a physical resistance or by a non-soluble lead compound in citrate solution. In accordance with these guesses two additional tests were carried out with different pretreatments: a dry milling (PT-3) and a sulphuric acid washing (PT-4). Dry milling was performed in a planetary mill with 20 balls (1mm in diameter), 450 rpm and 2 min, and the sulphuric acid washing was carried out in a 70 g/L sulphuric acid solution, magnetically stirred, at 85 ºC with 4% pulp density and a reaction time of 1 hour. After acid washing, the weight loss was of 63.4% due to the dissolution of jarosite and a part of gypsum. Pb extraction in PT-3 was similar to PT-1 and PT-2, while with a previous acid washing (PT-4) lead recovery reaches a high extraction, 96.4%. These results suggest that lead found in beaverite particles can not be dissolved in citrate solutions. To confirm this refractory behaviour some XRD analysis were performed (Fig. 4), Fig. 4A shows the XRD pattern of the citrate leaching residue where pyrite, quartz, hydronian jarosite and beaverite are found, anglesite and gypsum are mostly dissolved in the citrate leaching stage, therefore lead contained in beaverite structure is not leached. Instead, Fig. 4B presents the XRD pattern of solid obtained after the H_2SO_4 washing, where it can be observed that hydronian jarosite and beaverite are leached with this pre-treatment, and anglesite is the unique lead specie, enhancing the lead recovery, upper than 95%.

Table 4: experimental conditions and lead recovery in preliminary citrate leaching tests (1M sodium citrate and pH 7).

	PT-1	**PT-2**	**PT-3**	**PT-4**
Pretreatment	-	-	Dry milling	Sulphuric acid washing
Time (h)	2	16	2	2
Pulp density (%)	2	1	2	1.4
Pb recovery (%)	41.2	49.2	51.7	96.4

In view of these preliminary test results, a previous acid washing is proposed to reach higher lead recoveries in the citrate leaching stage. This acid washing dissolves jarosite and beaverite present in the bioleaching residue, releasing valuable metals, such as Pb or Ag, from jarosite structure (Sánchez et al., 1996) and keep the potential contaminants, like As or Fe, in solution. Fig. 5 shows the different routes to recover lead in citrate solution after the biooxidation processes, highlighting the benefits of introduce a previous stage of sulphuric acid washing.

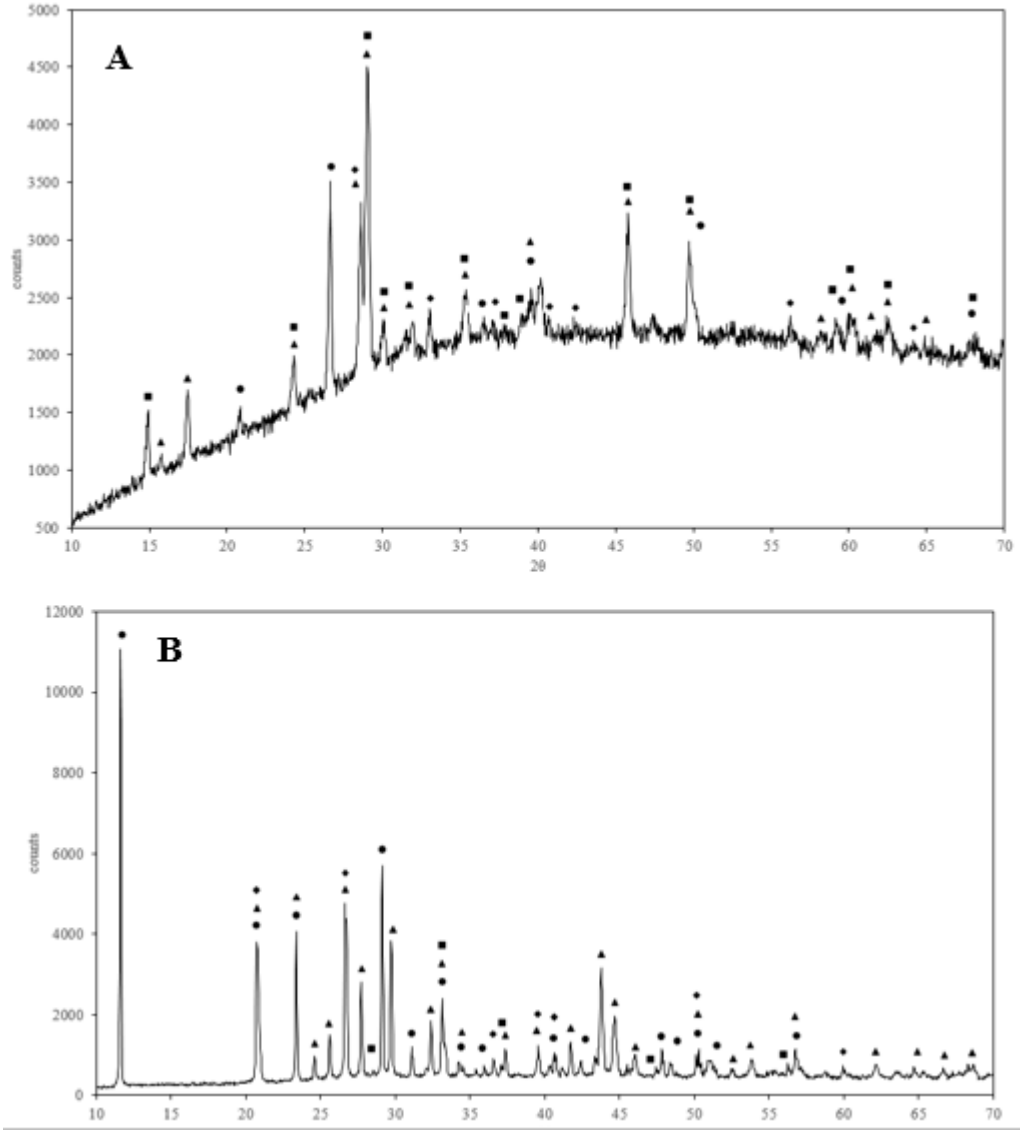

Fig. 4: XRD patterns of direct citrate leaching (1M, 2% pulp density, pH 7 and 2 h) (♦ = pyrite, ● = quartz, ▲ = hydronian jarosite and ■ = beaverite) (A), and acid washing residue (90 g/L H_2SO_4, 80 ºC, 1 h and 4% pulp density) (♦= Quartz, ■ = pyrite, ▲ = anglesite and ● = gypsum) (B).

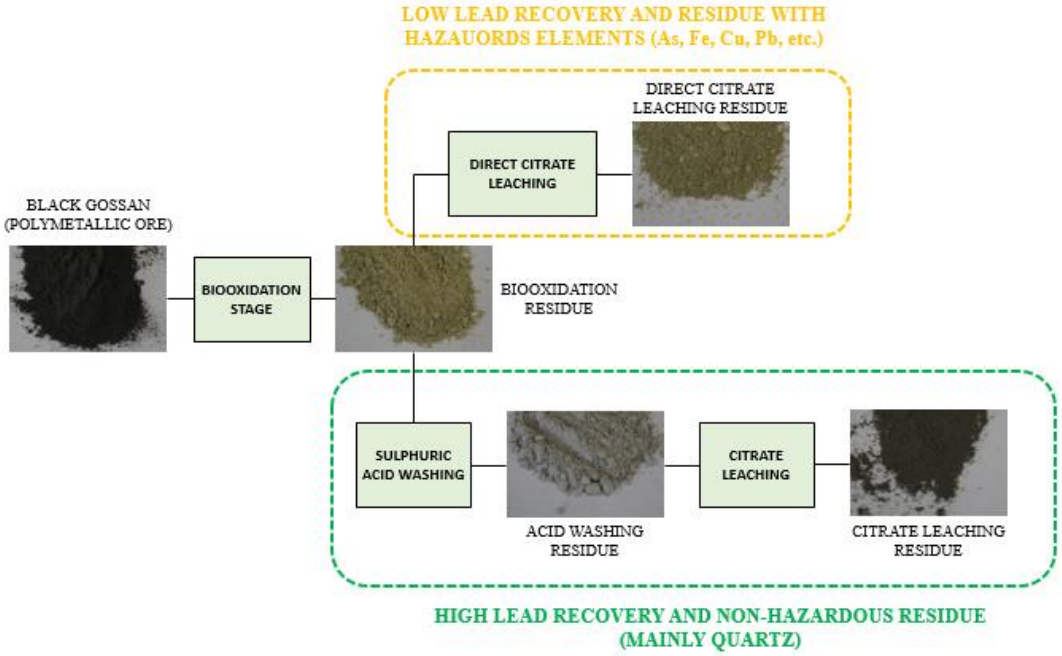

Fig. 5: Alternative routes to recover Pb, after bioleaching stage, through a citrate leaching.

3.2.2 Acid washing

In order to study the acid washing several experiments were performed using the biooxidation residue, where the effect of the sulphuric acid concentration, temperature, time and pulp density were tested.

Fig. 6A shows the jarosite dissolution at different sulphuric acid concentrations, in the range of 10-90 H_2SO_4 g/L. These results show a strong dependence of initial sulphuric acid concentration, varying the jarosite dissolution from 21.2 to 99.6% when the sulphuric acid concentration increased from 10 to 90 g/L. Also, a greater dependence of the sulphuric acid concentration can be observed at low concentrations (10-30 H_2SO_4 g/L).

According to Reyes et al. (2017), temperature plays a key role in the jarosite dissolution in sulphuric acid solutions. Fig. 6B presents the effect of temperature (50-80 ºC) in the jarosite dissolution. At 50 ºC jarosite dissolution is low (42%), however, when temperature increases upper 70 ºC, the jarosite dissolution reaches extractions higher than 90%: 90.1% at 70 ºC and 99.6% at 80 ºC.

The effect of reaction time is studied at different temperatures, in these tests different samples were withdrawn and filtered to obtain the jarosite dissolution as a function of

time. Fig. 6C shows the jarosite dissolution with respect time at different temperatures. Experiments carried out at 70 and 80 ºC have similar conversions after 60 min, although at early reaction times the test performed at 80 ºC has a higher rate. Instead, test realized at 60 ºC present a slower rate than the other tests, reaching a 75% of jarosite dissolution in 120 min.

To confirm the important role of time with respect temperature, the conversion-time curves obtained at different temperatures were adjusted at several kinetic equations (eqs. 3-5). The acidic dissolution of jarosite does not produce solid products on the unreacted jarosite particles, being the eq. 4 the best fitted kinetic equation (Fig. 6D). According with the Arrhenius equation (eq. 6), the activation energy is 86.5 kJ/mol, typical value for chemical reaction as the rate controlling step. Similar values, between 68 and 98.7 kJ/mol, have been found in literature in acid and basic medium, (Reyes et al., 2017).

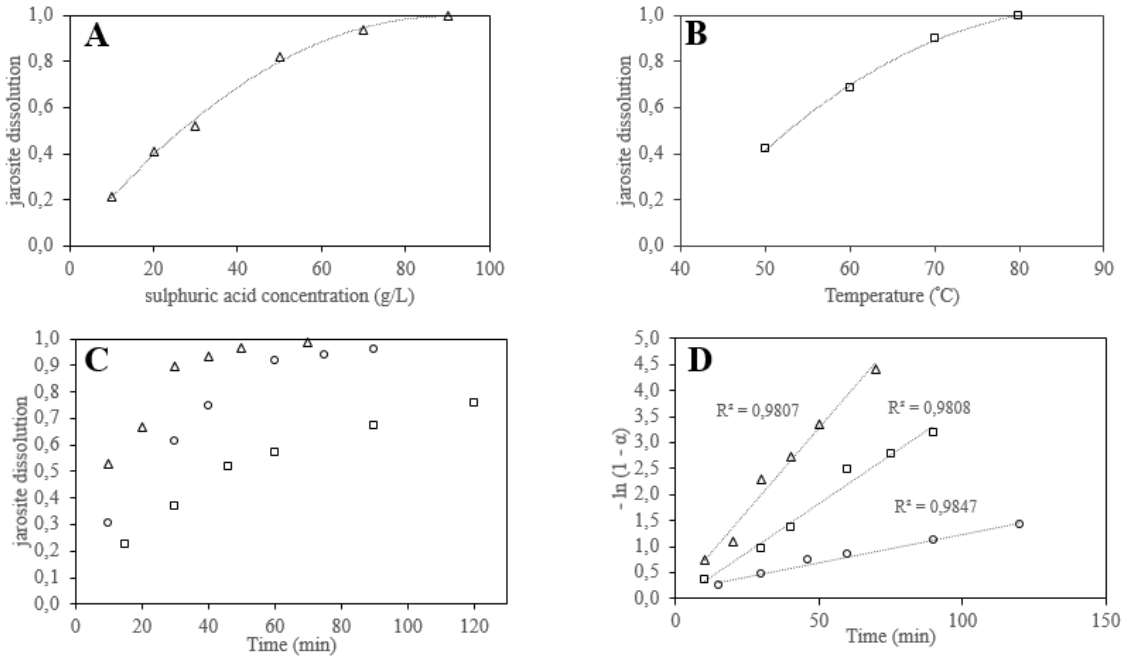

Fig. 6: jarosite dissolution as a function of sulphuric acid concentration (80 ºC, 4% pulp density and 1 h) (A); jarosite dissolution with respect temperature (90 g/L H_2SO_4, 1 h and 4% pulp density) (B); evolution of jarosite dissolution at different temperatures (4% pulp density and 90 g/L H_2SO_4) (□ = 60 ºC, ○ = 70 ºC and ▲= 80 ºC) (C); experimental data (○ = 60 ºC, □ = 70 ºC and ▲= 80 ºC) fit to eq. 4 (lines) (D).

With the aim of performing acid washing tests in a reactor with higher volume, several acid leaching experiments were carried out increasing the pulp density. Table 5 shows the jarosite dissolution at different times when pulp density increases to 8 and 12%. Longer reaction times are necessary to obtain conversions greater than 90%. At 8% pulp

density after 120 min jarosite dissolution is higher than 97%. Instead, at 12% pulp density the reaction rate is slow, reaching a conversion of 93% in 180 min. The lead solubility in citrate media was studied with the different residues obtained in these acid washing tests. Table 5 shows the lead recovery and the pretreatment conditions in each test. The experiments carried out at 12% pulp density reach Pb extractions lower than 95%, due to the low jarosite dissolution (93% in 180 min). In return, tests at 8% pulp density obtained lead recoveries upper than 95% in 120 minutes, 96% in 120 minutes and 97% in 180 minutes.

Table 5: Pb recovery in citrate leaching (1M, pH 7, 2 h and 2% pulp density) after sulphuric acid leaching at high pulp density (90 g/L and 80 ºC).

Pulp density in pretreatment (%)	**Pretreatment time (h)**	**Jarosite disolved (α)**	**Pb recovery in citrate stage (%)**
8	1	0.93	92.0
8	2	0.98	96.0
8	3	0.99	97.0
12	1	0.87	87.0
12	2	0.90	92.0
12	3	0.93	92.0

The chemical composition after the tests performed under optimal conditions in the stirred tank 6L-reactor is shown in Table 1, arsenic and iron from jarosite (hydronian jarosite and beaverite) are mostly dissolved and the main compounds in solid residue are gypsum and anglesite (Table 2). The chemical composition of liquors obtained is the following, being similar in both tests: 166.8 ± 1.0 ppm Cu, 18.6 ± 0.4 ppm Zn, 8002.0 ± 686.6 ppm Fe, 1.1 ± 0.1 ppm Co, 1.2 ± 0.1 ppm In, 314.0 ± 15.6 ppm Ca, 315.5 ± 13.6 ppm As and 59.4 ± 2.6 ppm Sb. The majority of metals (Cu, Fe or Zn) and As are removed in the dissolution, however Sb is partially dissolved remaining the greater part in the solid residue. The jarosite conversion obtained is 0.99.

3.2.3 Citrate leaching tests

3.2.3.1 Thermodynamic analysis

Some species distribution diagrams were performed with MEDUSA software (Puigdomenech, 2010) in order to observe the solubility zones of different metals that could form several complexes with citrate ion. Ion concentrations were selected according to concentration expected in test at 10% pulp density. Fig. 7 shows the species distribution diagram for Pb^{2+} (A), Ca^{2+} (B) and Fe^{3+} (C). The most stable lead-citrate complex is the $Pb(cit)_2^{4-}$ at pH range of 5-7.5. At pH lower than 4 the most stable lead specie is anglesite, and at pH higher than 9 lead hydroxide is the dominant compound. $CaSO_4 \cdot 2H_2O$ is the main compound in the acid washing residue, and a part of this one is dissolved in citrate media, the $Ca(cit)^-$ solubility enhances as pH increases. In tests carried out at low pulp densities gypsum is completely dissolved, but, if pulp density increases an important part of gypsum remains in the solid residue being able to cause solubility troubles in the solution. Last, iron, at very low concentration in this solid, could form various complexes as a function of pH.

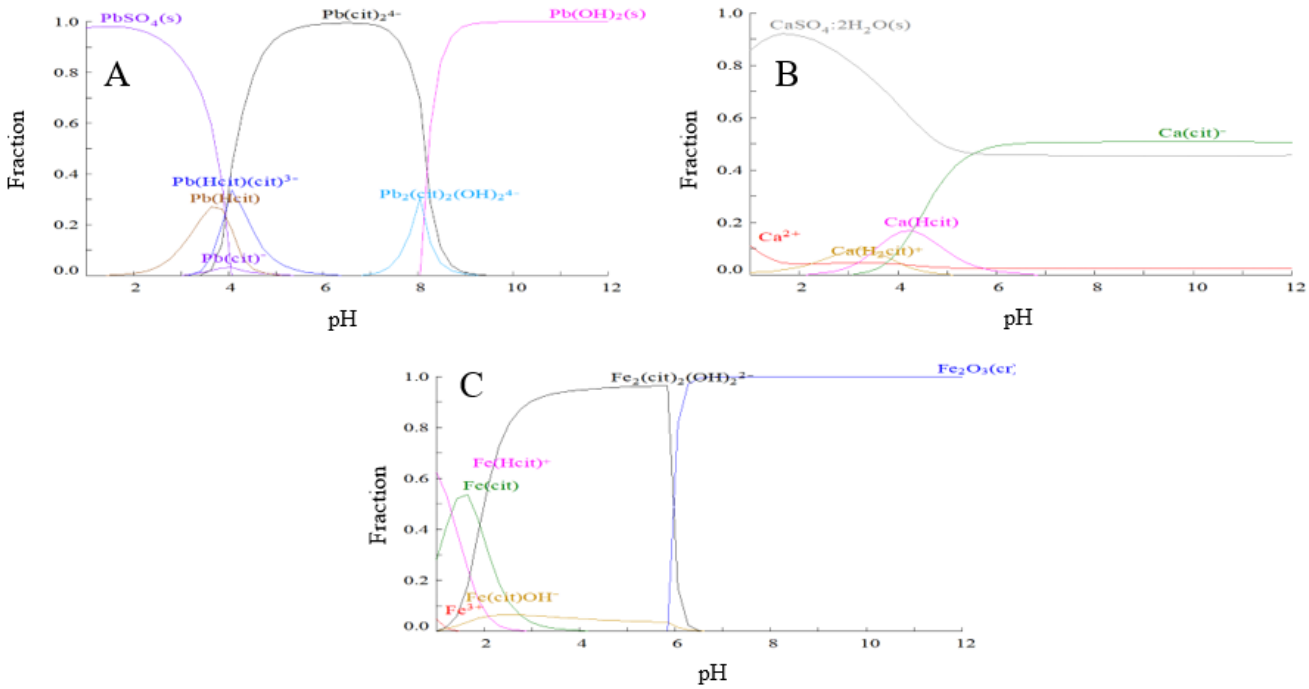

Fig. 7: (A) lead-citrate species distribution (1M citrate and 0.05M $PbSO_4$); (B) calcium-citrate species distribution (1M citrate and 0.4M $CaSO_4 \cdot 2H_2O$); (C) iron-citrate species distribution (1M citrate, 0.005M Fe^{3+} and 0.0075M SO_4^{2-}).

3.2.3.2 Citrate solution characterisation

In order to characterise the pregnant liquor solution (PLS) obtained in citrate tests, an experiment was performed with the following conditions: 1M sodium citrate, 2% pulp density, pH 7 and 2 hours. The stirred obtained was filtered and the solution was analysed by TXRF, technique that allows easily identify and quantify the elements presented in the sample. The solution was diluted with HCl. Pb, Ca, S and Fe were the principal elements determined, as well as, little amount of Cu, Zn and Sr. Ti was used as internal standard to quantify the concentration of elements present in solution (Table S1). Lead and calcium from anglesite and gypsum, respectively, are the main elements (anglesite and gypsum are completely dissolved in this test). A part of iron is dissolved in the citrate solution (< 50 ppm) producing a yellow complex (lead-citrate and calcium-citrate complexes are colourless). Copper and zinc concentration are almost negligible, close to 1 ppm. Ultimately, the sulphur presence is due to anglesite and gypsum dissolution, the accuracy of sulphur concentration measure is small due to the interferences produced by Mo k-radiation.

3.2.3.3 Effect of dissolved jarosite grade

Six citrate tests were carried out with acid washing residues, which have different grade of dissolved jarosite. Fig. 8 shows the linear relationship between the pre-treatment efficiency (jarosite dissolved) and the lead recovery in the citrate stage (R^2 = 0.999). This, joint to XRD analyses (Fig. 4), reinforces the hypothesis that a part of lead is found in the beaverite structure, playing the efficiency of jarosite dissolution (acid pre-treatment) a key role in the citrate leaching of lead.

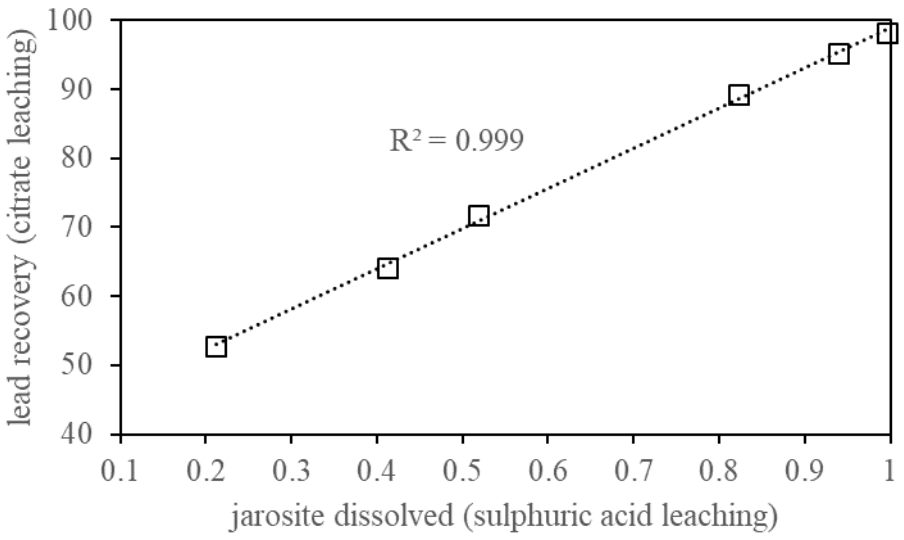

Fig. 8: Lead recovery as a function of dissolved jarosite (1M sodium citrate, 2h, pH 7, 2% pulp density).

3.2.3.4 Pulp density and pH effect

Pulp density and pH in the citrate leaching are studied in this section. As a function of pH different Pb-citrate complexes are formed. In the pH range of 5-7.5, lead presents the highest solubility in citrate solution. Instead, an increase of lead concentration induces to a shrinking in the solubility region, and a decrease in the lead dissolution rate (Zárate-Gutiérrez and Lapídus, 2014). Table 6 shows the lead recovery at different pulp densities and pHs. At pH 3 and 5% pulp density, Pb recovery is low (13.4%) due to the presence of $PbSO_4$, at this pH no Pb-citrate complexes are formed. Instead, in the pH range of 5-10.5 (at 5% pulp density), high lead recoveries were obtained (> 96%).

When pulp density was increased from 7.5 to 15%, different results were obtained. In the case of test performed at 7.5% of pulp density similar results with respect the above tests were achieved with the exception of test at pH 10.5, where the lead recovery decreased to 80%. This result is due to the deceleration in the kinetics and $Pb(OH)_2$ formation, in accordance with Zárate-Gutiérrez and Lapidus (2014). An important decrease of Pb extraction was observed at 10% pulp density and at higher pHs. At 15% of pulp density recoveries lower than 40% were achieved. At pulp densities > 7.5% a white precipitate is formed, the precipitation increases as pH and pulp density increase.

Table 6: Pb recovery as a function of pH and pulp density (%) (1 hour, 1M sodium citrate).

	pH				
p. d. (%)	3	5	7	9	10.5
5	13.41	**97.72 ± 0.99**	**97.50 ± 0.38**	**96.59± 1.68**	96.49
7.5	-	96.45	86.75	96.03	80.50
10	-	76.08	70.92	50.76	-
15	-	33.29	36.72	-	-

The lead solubility limit is not reached in these tests, however at pulp densities ≥7.5%, an unstable solution is obtained. Fig. 9A shows, as an example, the evolution of Pb concentration, at different pH, in liquors achieved in test performed at 7.5% pulp density. It can be observed that lead gradually precipitates, being the solubility greater at high pH. Besides, Fig. 9B shows the soluble Pb stability as a function of time and pH in tests performed at 5% pulp density, in this case liquor is stable and no precipitation is observed. Only in the case of pH 5 a precipitate is observed after 40 h. This unstable behaviour could be caused by the presence of large amounts of gypsum when pulp density goes up.

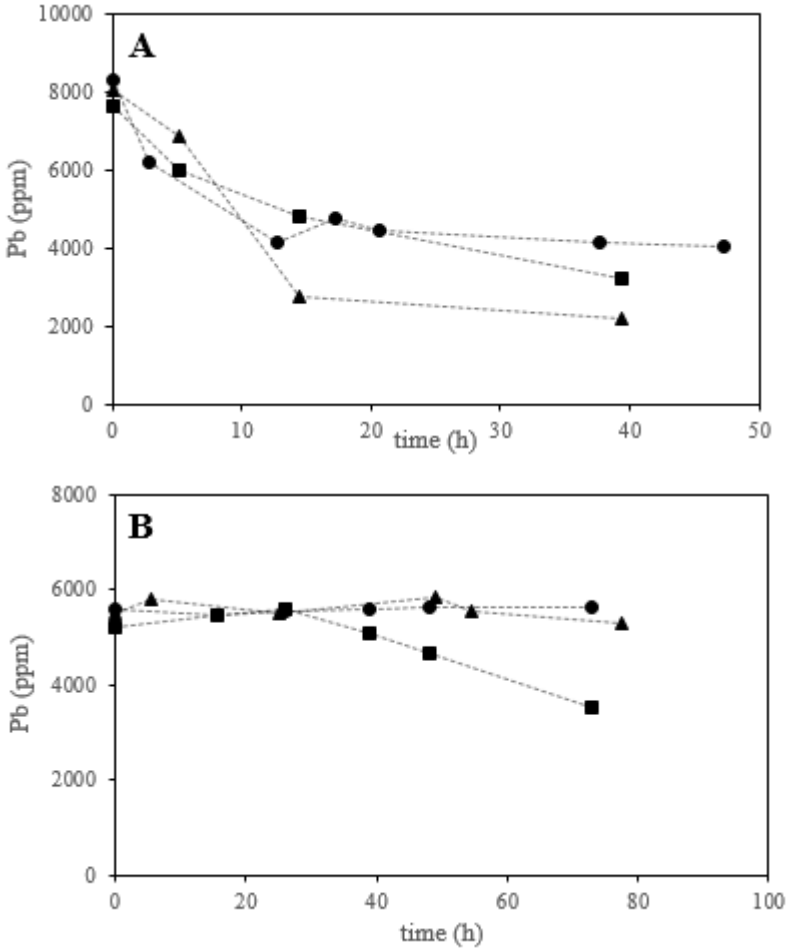

Fig. 9: Stability of lead remaining in solution at different pH. Solution obtained at 7.5% of pulp density (▲= pH 5, ■ = pH 7 and ● = pH 9) (A), and solution obtained at 5% of pulp density (■ = pH 5, ▲= pH 7 and ● = pH 9) (B).

Precipitates formed in different experiments were filtered, dried, dissolved in HCl and analysed by AAS and TXRF. The chemical composition of precipitates formed at different pH are similar, 8.6 ± 0.3% Pb and 12.8 ± 1.5 % Ca. The precipitate formed at 10% pulp density and pH 7 was analysed by XRD (Fig. S6), no crystalline species were identified. In the interest of identify the elements presents in the precipitate, a part of solid was dissolved in HCl media and analysed by TXRF. TXRF data shows the presence of Pb, Ca and a little amount of Fe. S was not identified. These measurements (XRD and TXRF) suggest that an insoluble calcium citrate is formed, co-precipitating a part of Pb.

In order to observe the reproducibility of these tests under optimal conditions (5% pulp density and pH range of 5-9) a duplicate in the optimal was performed, standard deviations (SD) obtained are shown in Table 6, in all cases a small SD is calculated.

3.2.3.5 Citrate leaching with pure anglesite and gypsum

With the aim to confirm the above guesses, various tests (with typical anglesite and gypsum amounts in tests at 7.5% pulp density) were carried out with pure anglesite (PANREAC) and gypsum synthesised from the calcium carbonate (FLUKA) and sulphuric acid (PANREAC) (r7 and r8). Tests carried out with pure anglesite reach the complete dissolution after 20 min of reaction, alternately when anglesite and gypsum were mixed a part of gypsum was not dissolved. Calcium extraction enhanced as pH increased. Fig. 10A shows the lead concentration with respect time, when only anglesite is added at different pH, it can be observed that the solution rich in lead is stable. However, in tests where gypsum is added (Fig 10B) the solution obtained is not stable and Pb precipitates gradually. Results when anglesite and gypsum are mixed are so similar to results obtained from tests performed at 7.5% pulp density (Fig. 9A), where liquor is not stable. Due to the negative effect of the gypsum presence, a decrease of the pulp density is suggested to recover lead from lead-bearing solids with large amounts of gypsum.

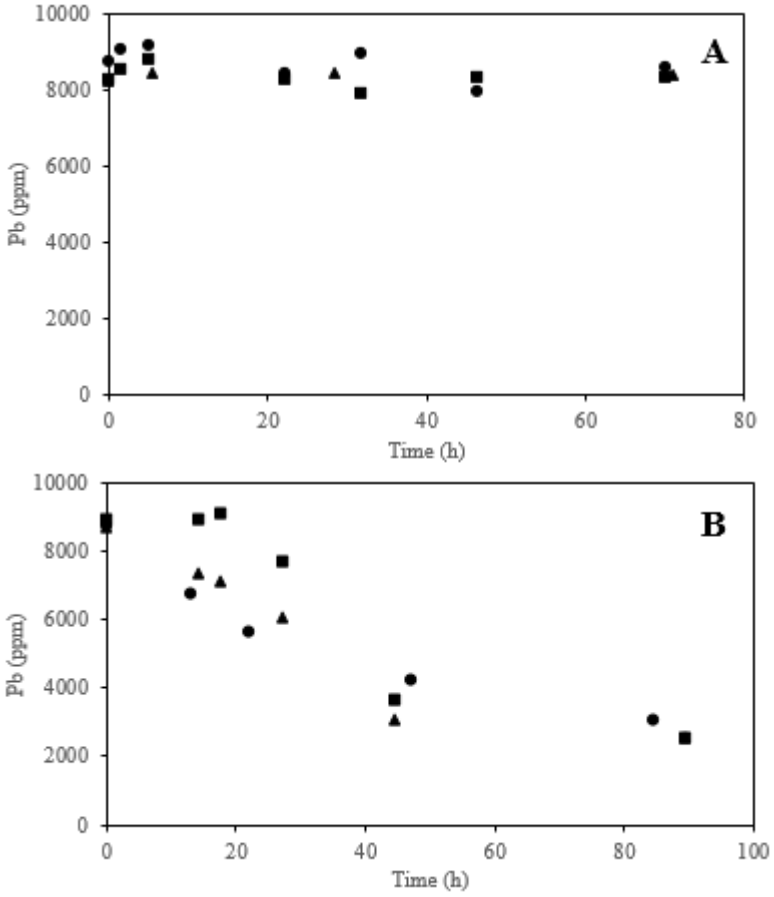

Fig. 10: Lead stability in citrate solution performed with pure anglesite (1 hour, 12.4 g/L $PbSO_4$, 1M sodium citrate) (■ = pH 5, ● = pH 7 and ▲ = pH 9) (A) and lead stability in citrate solution performed with pure anglesite and gypsum (1 hour, 12.4 g/L $PbSO_4$, 47.5 g/L $CaSO_4 \cdot H_2O$, 1M sodium citrate) (■ = pH 5, ▲ = pH 7 and ● = pH 9) (B).

3.2.3.5 Citrate leaching residue

The main specie in the final solid residue is quartz, with a minor proportion of pyrite. After biooxidation, acid washing and citrate leaching stages, the mean composition in Ag and Au in the residue is 1382 ± 22 ppm and 20.1 ± 0.3 ppm, respectively (Fig. 11). Gold and silver were liberated in the biooxidation, and in the acid washing the different elements, that could hinder the gold and silver recovery, were removed. The precious metals could be easily recovered in a subsequent stage.

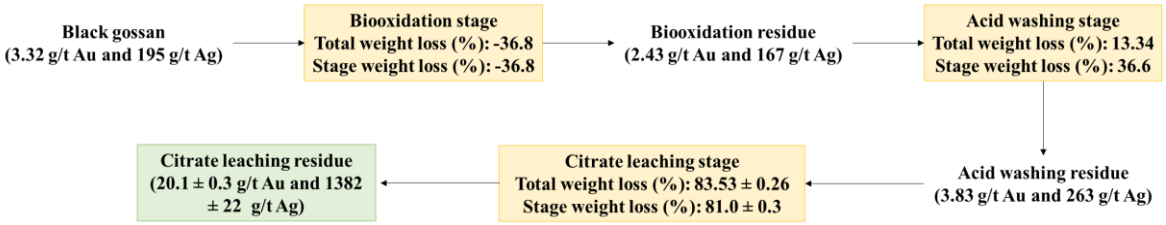

Fig. 11: Cumulative and stage weight loss in each stage and Ag and Au grade in residues obtained.

4. Conclusions

A novel cleaner process for the recovery of lead, silver and gold from sulphide ores has been studied. The biooxidation following by an acid washing and a citrate leaching is a satisfactory treatment for recover Pb and remove the refractoriness of sulphide ores rich in Pb, Ag and Au. The bioxidation stage is able to remove the refractory behaviour, increasing the gold extraction from 17.3 to 86.4% through a traditional cyanide leaching, and to oxidise the sulphides. A direct citrate leaching of the biooxidation residue reaches a low lead recoveries, but if hydronian jarosite and beaverite are dissolved through an acid washing the lead recovery increases from 41.2 to 96.4%. In this acid washing, temperature and sulphuric acid concentration are the mandatory variables, an activation energy of 86.4 kJ/mol was determined. A linear relationship between the jarosite dissolved and the lead recovery in the citrate leaching was found, playing the efficiency in the acid washing a key role in this alternative approach. Pulp density and pH are the most important variables in the citrate leaching, after acid washing. The optimal pH range was 5-9, a Ca-Pb-citrate precipitate is formed when pulp density is higher than 5%. In tests carried out with commercial anglesite, a negative effect of gypsum presence was observed. A precipitate similar to non-soluble compound produced in experiments with real solid was found. After the biooxidation treatment and the lead recovery stage, a solid residue, mainly composed of quartz, rich in gold and silver (liberated from sulphide matrix) was obtained. These precious metals could be easily benefited in a subsequent stage.

5. Acknowledgements

CLC Company supplied the black gossan. Thanks are given to Alberto Ortega-Galván (CITIUS) to perform and interpret the TXRF analyses.

6. References

Amankwah, R. K., Yen, W. T., & Ramsay, J. A. (2005). A two-stage bacterial pretreatment process for double refractory gold ores. Minerals engineering, 18(1), 103-108.

Behnajady, B., & Moghaddam, J. (2014). Optimization of lead and silver extraction from zinc plant residues in the presence of calcium hypochlorite using statistical design of experiments. Metallurgical and Materials Transactions B, 45(6), 2018-2026.

Brierley, C. L. (2008). How will biomining be applied in future?. Transactions of nonferrous metals society of China, 18(6), 1302-1310.

Celep, O., Alp, İ., & Deveci, H. (2011). Improved gold and silver extraction from a refractory antimony ore by pretreatment with alkaline sulphide leach. Hydrometallurgy, 105(3-4), 234-239.

Celep, O., Altinkaya, P., Yazici, E. Y., & Deveci, H. (2018). Thiosulphate leaching of silver from an arsenical refractory ore. Minerals Engineering, 122, 285-295.

Choi, N. C., Cho, K. H., Kim, B. J., Lee, S., & Park, C. Y. (2018). Enhancement of Au–Ag–Te contents in tellurium-bearing ore minerals via bioleaching. International Journal of Minerals, Metallurgy, and Materials, 25(3), 262-270.

Dunn, J. G., & Chamberlain, A. C. (1997). The recovery of gold from refractory arsenopyrite concentrates by pyrolysis-oxidation. Minerals Engineering, 10(9), 919-928.

Eymery, J. P., & Ylli, F. (2000). Study of a mechanochemical transformation in iron pyrite. Journal of alloys and compounds, 298(1-2), 306-309.

Fleming, C. A., McMullen, J., Thomas, K. G., & Wells, J. A. (2003). Recent advances in the development of an alternative to the cyanidation process: Thiosulfate leaching and resin in pulp. Minerals and metallurgical processing, 20(1), 1-9.

Fomchenko, N. V., Kondrat'eva, T. F., & Muravyov, M. I. (2016). A new concept of the biohydrometallurgical technology for gold recovery from refractory sulfide concentrates. Hydrometallurgy, 164, 78-82.

Frías, C., Díaz, G., Ocaña, N., & Lozano, J. I. (2002). Silver, gold and lead recovery from bioleaching residues using the PLINT process. Minerals Engineering, 15(11), 877-878.

Gomez, C., Limpo, J. L., De Luis, A., Blazquez, M. L., Gonzalez, F., & Ballester, A. (1997). Hydrometallurgy of bulk concentrates of Spanish complex sulphides: Chemical and bacterial leaching. Canadian metallurgical quarterly, 36(1), 15-23

Gudyanga, F. P., Mahlangu, T., Roman, R. J., Mungoshi, J., & Mbeve, K. (1999). An acidic pressure oxidation pre-treatment of refractory gold concentrates from the Kwekwe roasting plant, Zimbabwe. Minerals Engineering, 12(8), 863-875.

Hasab, M. G., Rashchi, F., & Raygan, S. (2013a). Simultaneous sulfide oxidation and gold leaching of a refractory gold concentrate by chloride–hypochlorite solution. Minerals Engineering, 50, 140-142.

Hasab, M. G., Raygan, S., & Rashchi, F. (2013b). Chloride–hypochlorite leaching of gold from a mechanically activated refractory sulfide concentrate. Hydrometallurgy, 138, 59-64.

Hasab, M. G., Rashchi, F., & Raygan, S. (2014). Chloride–hypochlorite leaching and hydrochloric acid washing in multi-stages for extraction of gold from a refractory concentrate. Hydrometallurgy, 142, 56-59.

Iglesias, N., & Carranza, F. (1994). Refractory gold-bearing ores: a review of treatment methods and recent advances in biotechnological techniques. Hydrometallurgy, 34(3), 383-395.

Jeffrey, M. I., Breuer, P. L., & Choo, W. L. (2001). A kinetic study that compares the leaching of gold in the cyanide, thiosulfate, and chloride systems. Metallurgical and Materials Transactions B, 32(6), 979-986.

Kaksonen, A. H., Mudunuru, B. M., & Hackl, R. (2014). The role of microorganisms in gold processing and recovery—A review. Hydrometallurgy, 142, 70-83.

Kasaini, H., Kasongo, K., Naude, N., & Katabua, J. (2008). Enhanced leachability of gold and silver in cyanide media: Effect of alkaline pre-treatment of jarosite minerals. Minerals Engineering, 21(15), 1075-1082.

Kim, E., Horckmans, L., Spooren, J., Broos, K., Vrancken, K. C., & Quaghebeur, M. (2017). Recycling of a secondary lead smelting matte by selective citrate leaching of valuable metals and simultaneous recovery of hematite as a secondary resource. Hydrometallurgy, 169, 290-296.

Mahmoud, A., Cézac, P., Hoadley, A. F., Contamine, F., & D'Hugues, P. (2017). A review of sulfide minerals microbially assisted leaching in stirred tank reactors. International Biodeterioration & Biodegradation, 119, 118-146.

Melashvili, M., Fleming, C., Dymov, I., Matthews, D., & Dreisinger, D. (2016). Dissolution of gold during pyrite oxidation reaction. Minerals Engineering, 87, 2-9.

Mubarok, M. Z., Winarko, R., Chaerun, S. K., Rizki, I. N., & Ichlas, Z. T. (2017). Improving gold recovery from refractory gold ores through biooxidation using iron-sulfur-oxidizing/sulfur-oxidizing mixotrophic bacteria. Hydrometallurgy, 168, 69-75.

Nesbitt, C.C., Milosavljevic, E.B., Hendrix, J.L., 1990. Determination of the mechanism of the chlorination of gold in aqueous solutions. Industrial & Engineering Chemistry Research 29, 1696–1700.

Norgate, T., & Jahanshahi, S. (2010). Low grade ores–smelt, leach or concentrate?. Minerals Engineering, 23(2), 65-73.

Palencia, I., Carranza, F., & Garcia, M. J. (1990). Leaching of a copper-zinc bulk sulphide concentrate using an aqueous ferric sulphate dilute solution in a semicontinuous system. Kinetics of dissolution of zinc. Hydrometallurgy, 23(2-3), 191-202.

Patiño, F., Viñals, J., Roca, A., & Núñez, C. (1994). Alkaline decomposition-cyanidation kinetics of argentian plumbojarosite. Hydrometallurgy, 34(3), 279-291.

Puigdomènech, I. (2010). Make equilibrium diagrams using sophisticated algorithms (MEDUSA), software version 18 February 2004. Inorganic Chemistry Department, Royal Institute of Technology, Stockholm, Sweden. Available from:< http://web. telia. com/~ u15651596/>(consulted 05.10. 07).

Reyes, I. A., Patiño, F., Flores, M. U., Pandiyan, T., Cruz, R., Gutiérrez, E. J., & Flores, V. H. (2017). Dissolution rates of jarosite-type compounds in H2SO4 medium: A kinetic analysis and its importance on the recovery of metal values from hydrometallurgical wastes. Hydrometallurgy, 167, 16-29.

Sanchez, L., Cruells, M., & Roca, A. (1996). Sulphidization-cyanidation of jarosite species: Applicability to the gossan ores of Rio Tinto. Hydrometallurgy, 42(1), 35-49.

Schippers, A., Hedrich, S., Vasters, J., Drobe, M., Sand, W., & Willscher, S. (2013). Biomining: metal recovery from ores with microorganisms. In Geobiotechnology I (pp. 1-47). Springer, Berlin, Heidelberg.

Silverman, M.P. and Lundgren, D. G. (1959). Studies on the chemoautotrophic iron bacterium Ferrobacillus ferrooxidans. I. An improved medium and a harvesting procedure for securing high cell yields. J Bacteriol. 77(5):642-7.

Sonmez, M. S., & Kumar, R. V. (2009). Leaching of waste battery paste components. Part 2: Leaching and desulphurisation of PbSO4 by citric acid and sodium citrate solution. Hydrometallurgy, 95(1-2), 82-86.

Tornos, F., Velasco, F., Menor-Salván, C., Delgado, A., Slack, J. F., & Escobar, J. M. (2014). Formation of recent Pb-Ag-Au mineralization by potential sub-surface microbial activity. Nature communications, 5, 4600.

Viñals, J., Nunez, C., & Carrasco, J. (1991). Leaching of gold, silver and lead from plumbojarosite-containing hematite tailings in HCl CaCl2 media. Hydrometallurgy, 26(2), 179-199.

Webster, J. G. (1984, October). Thiosulphate complexing of gold and silver during the oxidation of a sulphide-bearing carbonate lode system, upper ridges mine. In PNG Gold-Mining, Metallurgy and Geology Conference, Australia (pp. 1-9).

Xu, B., Yang, Y., Li, Q., Jiang, T., & Li, G. (2016). Stage leaching of a complex polymetallic sulfide concentrate: Focus on the extraction of Ag and Au. Hydrometallurgy, 159, 87-94.

Zárate-Gutiérrez, R., & Lapidus, G. T. (2014). Anglesite (PbSO4) leaching in citrate solutions. Hydrometallurgy, 144, 124-128.

Zhang, W., Yang, J., Hu, Y., He, X., Zhu, X., Kumar, R. V. & Hu, J. (2016). Effect of pH on desulphurization of spent lead paste via hydrometallurgical process. Hydrometallurgy, 164, 83-89.

Zhu, X., He, X., Yang, J., Gao, L., Liu, J., Yang, D. & Kumar, R. V. (2013). Leaching of spent lead acid battery paste components by sodium citrate and acetic acid. Journal of hazardous materials, 250, 387-396.